Available online at www.sciencedirect.com
SCIENCE DIRECT®
PERGAMON
Radiation Measurements 37 (2003) 595–601
Radiation Measurements
www.elsevier.com/locate/radmeas

Calculations of track parameters and plots of track openings and wall profiles in CR39 detector

D. Nikezic[1], K.N. Yu*

Department of Physics and Materials Science, City University of Hong Kong, Tat Chee Avenue, Kowloon Tong, Kowloon, Hong Kong

Accepted 28 April 2003

Abstract

Computer programs have been developed to calculate track parameters and to plot track openings and wall profiles. The programs are based on equations derived for three-dimensional consideration of track development. All possible cases of track openings and wall profiles are obtainable from these equations. Results are given for lengths of major and minor axes, track depths and surface areas of track openings. Some examples of track openings and wall profiles are also presented.

Keywords: Solid state nuclear track detectors; CR39; Track parameters

1. Introduction

Equations for the walls and openings for tracks (etch-pits) in all phases of development have been derived by Nikezic and Yu (2003). Three-dimensional analytical consideration of track development was used to derive those equations. The objective of the present work is to study whether the equations can be used to calculate track parameters and to plot track openings and wall profiles.

The equations were incorporated into computer programs which enabled the following: plotting the track opening contour lines and the track wall profiles, calculations of the lengths of the major and minor axes, the track depths and the surface areas of the track openings. For completeness, the most important equations derived previously will be presented below, but without the derivations.

1.1. Sharp phase

In this phase of track development, the etching solution does not reach the particle range in the detector. The track tip is sharp and the track wall has a semi-conical profile (the track will be a regular cone if the track-etch rate V_t is constant). The coordinates (x, y) of a point on the track wall in two dimensions can be calculated from

$$x = x_0 + B \sin \delta(x_0), \tag{1}$$

$$y = B \cos \delta(x_0), \tag{2}$$

$$B = V_b(T - t_0), \tag{3}$$

where T is the total etching time, V_b the bulk etch rate, t_0 the time when the etchant reaches the point x_0 in the particle trajectory, and $\delta(x_0)$ is the local developing angle at point x_0 which is given by $\delta(x_0) = \mathrm{a}\sin(1/V(x_0))$ with

$$V = V_t(x_0)/V_b, \tag{4}$$

where $V_t(x)$ is the track etch rate at the point with coordinate x along the particle track. By using Eqs. (1)–(4), the coordinates of the points on the track wall can be generated. A best fit will give

$$y \approx F(x, L). \tag{5}$$

The equation of the track wall in the conical phase in three dimensions for normal incidence is given as

$$\sqrt{x^2 + y^2} = F(z, L), \tag{6}$$

where the z-axis is along the particle trajectory, and (x, y) are coordinates of points on the track wall (Nikezic and Yu, 2003). The track opening is circular in shape for normal

* Corresponding author. Tel.: +852-2788-7812; fax: +852-2788-7830.
E-mail address: peter.yu@cityu.edu.hk (K.N. Yu).
[1] On leave from Faculty of Sciences, University of Kragujevac, 34000 Kragujevac, Yugoslavia.

1350-4487/03/$ - see front matter
doi:10.1016/S1350-4487(03)00080-5

incidence, but some egg-like shape, or droplet-like shape, or even more complicated shape for oblique incidence. The equation for the contour line of the track opening for an oblique incidence is given as

$$\sqrt{x''^2 + y''^2 \sin^2\theta} = F(y'' \cos\theta + h/\sin\theta, L), \quad (7)$$

where θ is the incident angle (with respect to the surface of the detector), (x'', y'') are coordinates of points on the track opening contour (the double quotes are used to make a distinction from (x, y) in Eq. (6)) and h is the thickness of the removed layer.

It is noted that the previous equations are valid for $L < R$, where R is the particle range in the detector. The tracks where etching passes the end point of the particle will be treated differently.

1.2. Over-etched phase

The equation for the track wall in the over-etched phase for normal incidence in two dimensions is

$$y = F(z - d\sin\delta, R) + d\cos\delta, \quad (8)$$

where d is the over-etched thickness, i.e., the removed layer after the etching solution passes the particle range, and $\delta = a\sin(1/V(\xi))$ is the local developing angle of the track.

The equation of the track wall (also for normal incidence) in three dimensions is given analogously to Eq. (6) as

$$\sqrt{x^2 + y^2} = F(z - d\sin\delta, R) + d\cos\delta. \quad (9)$$

The equation of the contour line of the opening for an oblique incident angle θ was derived as

$$\sqrt{x''^2 + y''^2 \sin^2\theta} = F(y'' \cos\theta + z_0 - d\sin\delta, R) + d\cos\delta, \quad (10)$$

where (x'', y'') are, again, coordinates of points on the contour line of the track opening.

2. Short description of the program

Based on the above equations, we have developed computer programs to calculate track parameters. Programs were written in the standard FORTRAN90 language, and made use of graphic functions, subroutines and graphic modules from Microsoft® Fortran PowerStation® (version 4). The graphic routines enabled plotting the track profiles and contour lines. There are a number of programs, each dealing with different tasks. The first program, called TRAG.F90, is the most important one. Calculations in this program were performed with the following steps:

(a) reading input parameters: incident energy E_α and incident angle θ of alpha particles, removed thickness h and bulk etch rate V_b;
(b) determination of the alpha particle range R in the detector (CR39 detector in the present study) using the SRIM2000 program;
(c) determination of the distance L to which the etching solution penetrates along the particle track: Eqs. (1)–(7) used for $L < R$, and Eqs. (8)–(10) used otherwise;
(d) generating output files: a set of coordinates for points on the track wall. Based on these sets of data, the program calculates the length of the major axis of the opening, as well as the track depth.

The second program, called CONTOUR.F90 is used to calculate the coordinates (x'', y'') of the opening contour (based on the equation given above and the geometrical condition of the track). It generates an output file that contains the calculated coordinates. The minor axis and the area of the track opening are calculated by this program.

The third program, DRAW1.F90, was used for graphical presentation of the track profile and contour of the opening. This program imports data from the output files generated by TRAG.F90 and CONTOUR.F90, and simply draws the lines from one point to the contiguous point, creating the track profile or contour line. The coordinate system is chosen to match the computer screen so that the obtained images represent real-world appearances. In other words, ratios between parameters also represent the real-world figures. Some standard commercially available graphic softwares, like Microcal™ ORIGIN® or SPSS® SIGMAPLOT®, can also be used for graphical presentation of the track and opening shape. However, the images can be distorted in these cases and ratios of the parameters in the figure might not be the same as those in the real world.

3. Results

The programs mentioned above and Eqs. (1)–(10) were used for systematical studies of variations of track parameters with the incident angles and energies of the alpha particles. We have chosen to study detection of alpha particles with the CR39 detector in the present investigation. The incident angle was varied from 10° to 90° with steps of 10° while the incident energy was varied with steps of 1 MeV. All calculations were performed for a removed layer of 20 μm.

The function $V(R')$ was chosen as

$$V = 1 + (11.45e^{-0.339R'} + 4e^{-0.044R''})(1 - e^{-0.58R'}), \quad (11)$$

where R' is the residual range (Durrani and Bull, 1987). Other expressions for the function can also be employed.

3.1. Major axis

The results for the major-axis lengths are given in Fig. 1. The major-axis length increases initially with energy but decreases afterwards. The location of the curve

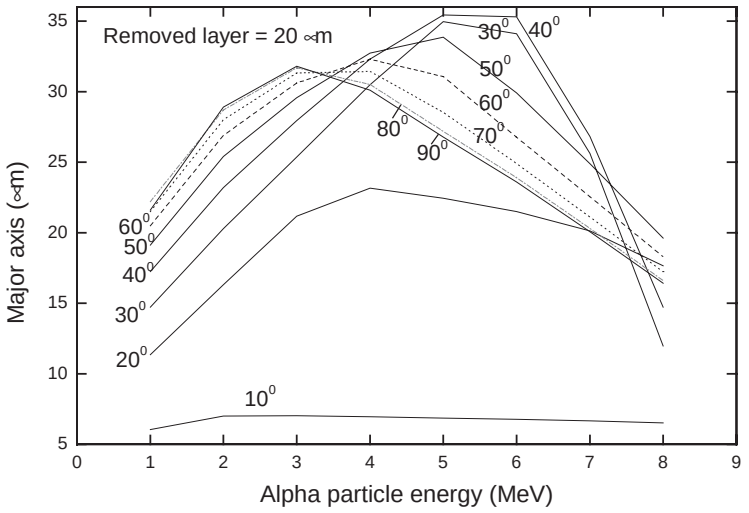

Fig. 1. Relationship between the major-axis length and the incident alpha particle energy, with the incident angle as a parameter.

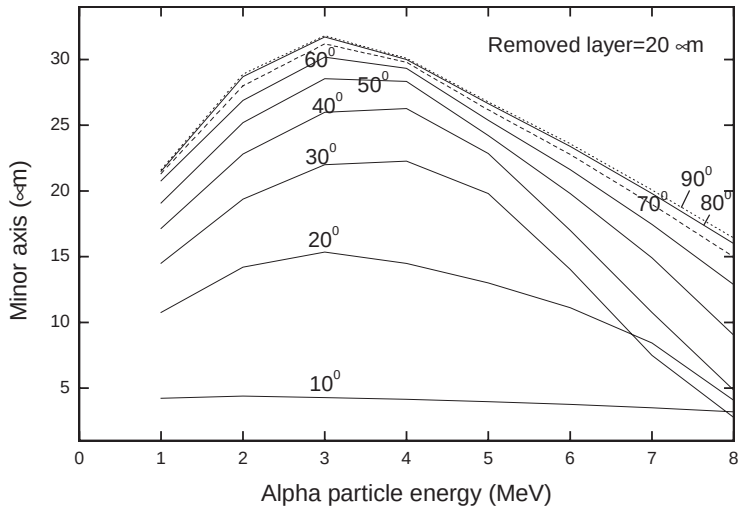

Fig. 2. Relationship between the minor-axis length and the incident alpha particle energy, with the incident angle as a parameter.

maximum in Fig. 1 depends on the incident angle of the alpha particle. In fact, the major-axis length depends on the incident energy and angle of the alpha particle in a very complicated way. The same length can be obtained for different combinations of incident angles and energies. Furthermore, some curves in Fig. 1 are very close to each other. For example, there is no significant difference between the curves for incident angles of 80° and 90°. Therefore, determination of incident energy or angle of alpha particles based on the major axis alone can be unrealistic.

3.2. Minor axis

The results for the minor-axis lengths are given in Fig. 2. The minor-axis length also increases initially with energy and then decreases in the higher-incident-energy region. However, the relationship between the minor-axis length and the incident angle is less complicated than the case for the major axis. For example, the curves in Fig. 2 have much fewer intersections than those in Fig. 1. The minor-axis length also increases monotonically with the incident angle of the alpha particle. Nevertheless, the curves for incident angles larger than 60° are also close to each other.

3.3. Surface area of track opening

The surface area of a track opening was calculated by numerical integration of the curve representing the track opening. Fig. 3 shows the relationship between the surface area of the track opening (in μm^2) and the incident energy of

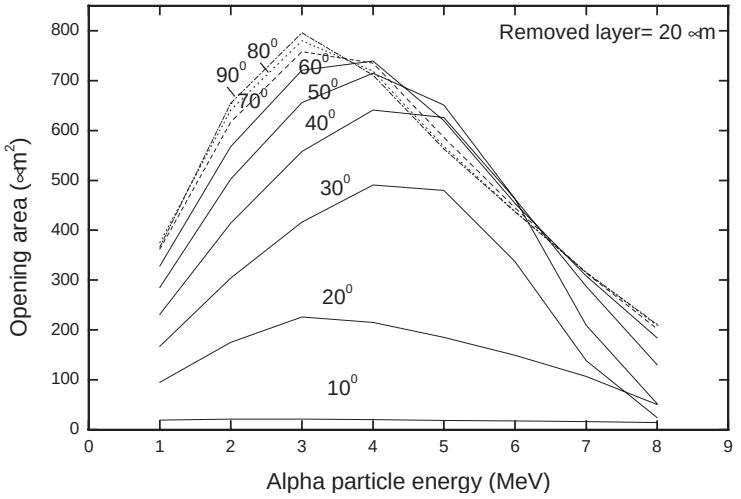

Fig. 3. Relationship between the surface-opening area and the incident alpha particle energy, with the incident angle as a parameter.

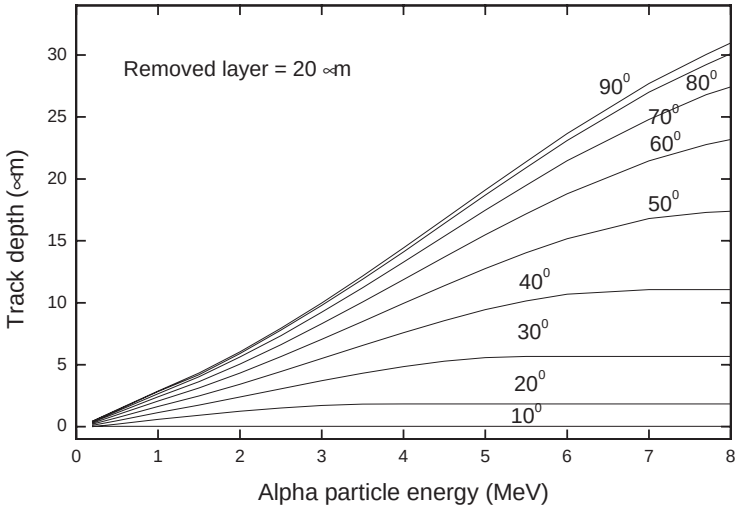

Fig. 4. Relationship between the track depth and the incident alpha particle energy, with the incident angle as a parameter.

the alpha particle. The area also increases initially and then decreases with the incident energy. For very small incident angles (10°), the surface area is almost independent of the incident energy. Dependence of the surface area on the incident energy is more pronounced for larger incident angles. The curves for incident angles larger than 60° are close to each other, which means the surface area weakly depends on the incident angle when the angle becomes large. This phenomenon is in fact desirable for alpha spectroscopy with the CR39 detector.

3.4. Track depth

The track depth dependence on the incident energy and angle are illustrated in Fig. 4. It can be observed that the track depth increases monotonically with the incident energy and angle of the alpha particle. There are no intersections at all among the curves for various incident angles. For smaller incident angles, the track depth can achieve saturation with increasing incident energy. For example, the track depth for incident angle of 30° flattens off for incident energies larger than 5 MeV. The saturation is related to the tracks whose developments do not begin at the original detector surface.

3.5. Track opening and track wall profile

Examples of predicted track profile and opening are shown in Figs. 5 and 6, respectively. The graphics are not perfect because they are produced directly

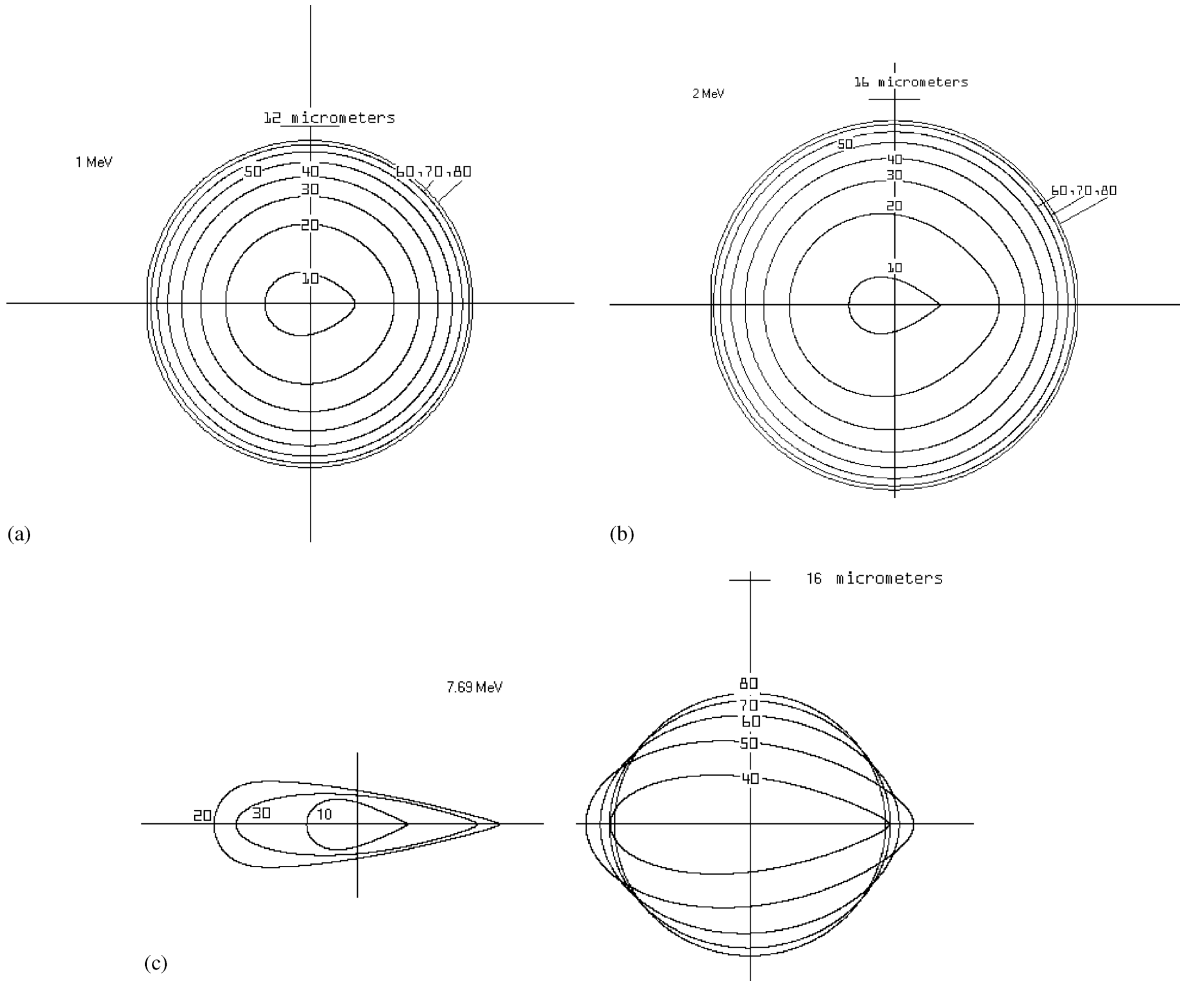

Fig. 5. Predicted track openings for alpha particles with different incident energies with the incident angle as a parameter. Incident energy: (a) 1 MeV, (b) 2 MeV and (c) 7.69 MeV.

from the FORTRAN program. However, with suitable scaling, the graphs can be used to recalculate realistic track dimensions of interest or to compare with direct measurements. For these purposes, the length marks on the ordinate axis at 2, 4, 12 or 16 μm should be employed.

Figs. 5(a)–(c) show predicted track openings for three different incident alpha particles energies (1, 2 and 7.69 MeV) and for incident angles between 10° and 80° with steps of 10° (the results for 90° is omitted here because they are completely circular and very close to the curve for 80°). All possible shapes of track openings are seen in these figures. Completely circular tracks are typical for large incident angles while very extended (not regular) elliptical or even more complicated shapes are typical for small oblique incident angles. The shape of the opening is more dependent on the incident angle than on the incident energy. For incident angles larger than 60°, the tracks are almost always circular in shape regardless of the incident energy (for the considered removed layer of 20 μm). Fig. 5(c) has two panels, the left one for the incident angles of 10°, 20° and 30°, while the right one for other angles (the lines will be too close to each other if shown in a single figure).

Figs. 6(a)–(c) show the predicted track wall profiles (in two dimensions) for three different incident alpha particle energies (3, 6 and 7.69 MeV) and for incident angles from 10° to 90° with steps of 10°. Again, the marks on the ordinate axis at 2 or 4 μm can be used to regenerate realistic track dimensions. Different phases of track development are seen in Figs. 6(a)–(c). Spherical and shallow tracks are typical for small incident energies and small incident angles, while tracks with sharp tips are typical for larger incident energies (7.69 MeV).

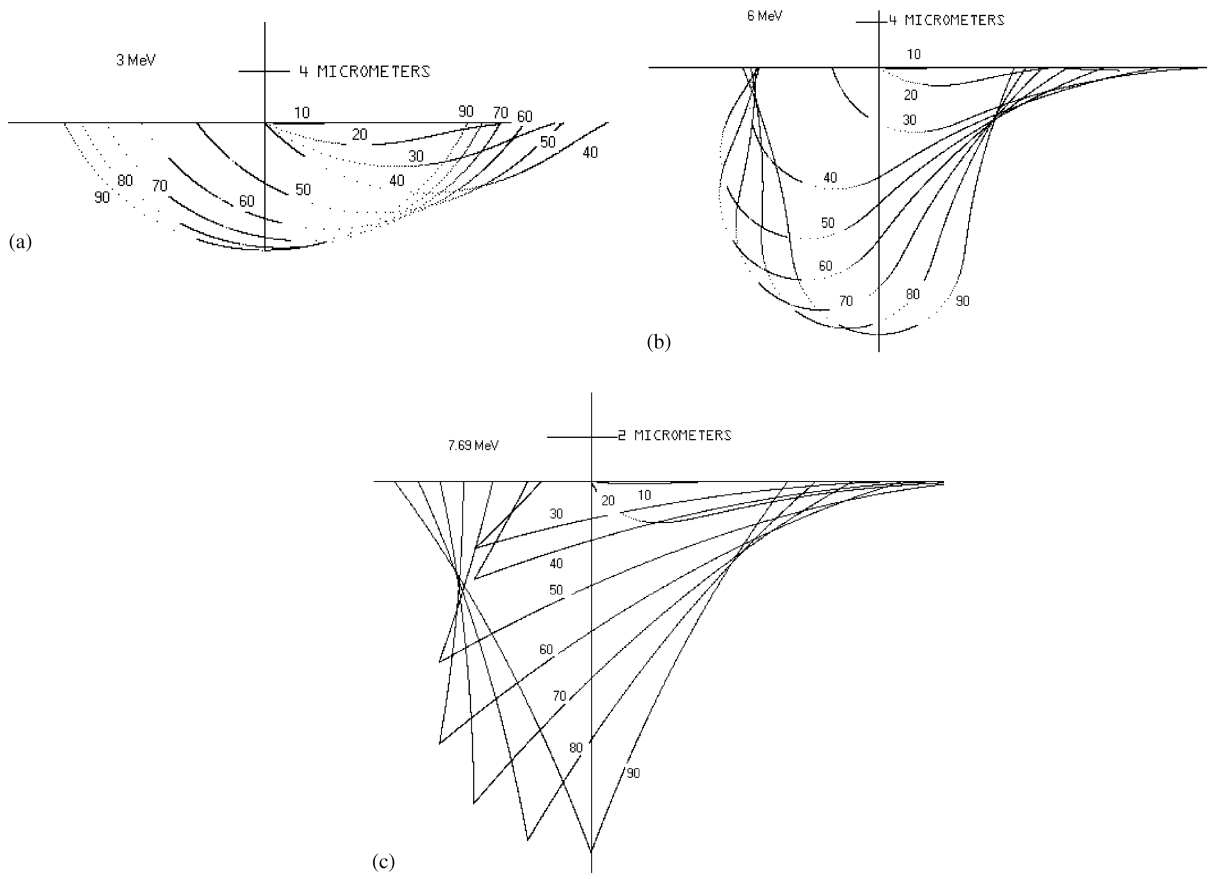

Fig. 6. Predicted track-wall profiles for alpha particles with different incident energies with the incident angle as a parameter. The removed layer was 20 μm. Dotted lines are used for better visibility. Incident energy: (a) 3 MeV, (b) 6 MeV and (c) 7.69 MeV.

4. Conclusions

Equations for track wall profiles and track openings derived previously were used to develop computer programs to study the tracks and to calculate their parameters. Examples of predicted track profiles and calculated tracks parameters confirm the applicability of these equations. All possible phases of track profiles and track openings are covered by these equations, which are seen in Figs. 5 and 6. Different cases of track openings have been considered in detail and plotted by Somogyi and Almasi (1979), and Somogyi and Szalay (1973). Their model was related to a constant V_t and specific expressions were derived for track parameters in each phase of the development. Criteria for transition from one phase to another were also given. However, our model is not based on such criteria, and the criteria are not even needed. The only condition needed to be examined for our model was whether etching passed the ending point of the particle range in the detector. Eqs. (1)–(10) have fully described the development of the track profile and the track opening.

Figs. 1–4 show that determination of the alpha particle energy is not possible if only one track parameter is considered. All track parameters depend on the incident energy and angle of the alpha particle in such a way that a combination of the parameters is needed to determine the incident alpha particle energy. It is also noted that some authors proposed the use of average gray level of the track as an additional parameter for alpha spectroscopy (Izerrouken et al., 1999; Skvarc, 1999), which might also be incorporated into our model.

Acknowledgements

The present research is supported by the CERG grants CityU1081/01P and CityU1206/02P from the Research Grant Council of Hong Kong.

References

Durrani, S.A., Bull, R.K., 1987. Solid State Nuclear Track Detection: Principles, Methods and Applications. Pergamon Press, Oxford.

Izerrouken, M., Skvarc, J., Ilic, R., 1999. Low energy alpha particle spectroscopy using CR-39 detector. Radiat. Meas. 31, 141–144.

Nikezic, D., Yu, K.N., 2003. Three-dimensional analytical determination of the track parameters. Over-etched tracks. Radiat. Meas. 37, 39–45.

Skvarc, J., 1999. Optical properties of individual etched tracks. Radiat. Meas. 31, 217–222.

Somogyi, G., Almasi, G., 1979. Etch pit formation in thin foils and a conductometric study of hole parameters. Proceedings of the 10th Solid State Nuclear Track Detectors, Lyon, France, 2–6 July 1979, pp. 257–266.

Somogyi, G., Szalay, A.S., 1973. Track diameter kinetics in dielectric track detector. Nucl. Instrum. Methods 109, 211–232.